# Visualization of Local Movements for optimal Marker Positioning

Ronan Boulic[1], Marius-Călin Silaghi[2], and Daniel Thalmann[1]

[1] Computer Graphics Lab, Swiss Federal Institute of Technology Lausanne, CH-1015 Lausanne Switzerland
{Ronan.Boulic,Daniel.Thalmann}@epfl.ch
[2] Artificial Intelligence Lab, Swiss Federal Institute of Technology Lausanne, CH-1015 Lausanne Switzerland
Marius.Silaghi@epfl.ch

**Abstract.** Motion Capture has been adopted for the production of highly realistic movements, as well as for the clinical analysis of pathological motions. In both cases, a skeleton model has to be identified to derive the joint motion. The optical technology has gained a large popularity due to the high precision of its marker position measurements. However, when it comes to building the skeleton frames out of the 3D marker positions, significant local skin deformations may penalize the quality of the model reconstruction. In this paper we exploit a local fitting tool to visualize the influence of skin deformation on marker movements. Such a knowledge can in turn improve the layout of optical markers. We illustrate our viewpoint on motions of the upper-torso.

## 1 Introduction

Various motion capture technologies are used for measuring the movement of human beings either for animating virtual humans or analysing the movement per se (e.g. for sport performance or clinical context). Until now, the most successful technology is optical motion capture. This is due to its high precision measurement of little reflective markers, attached on some relevant body landmarks. In a production context, the movement of an artist is captured with two to eight calibrated cameras. For simple motions, the multiple views of markers allow the automatic reconstruction of their 3D position. Depending on the system, a static posture [1] or a special calibration motion (further referred to as the *gym* motion) is used to build or adjust a skeleton model. The skeleton model helps, in a second phase, to derive the angular trajectories of all the captured motions. In this second phase, the markers are generally assumed to be fixed in the coordinate system of a body segment. This assumption is weak for a body region undergoing large deformations, such as the shoulder. In this paper we exploit a recent tool for the analysis of local marker displacements (i.e. with respect to the underlying bones). This tool is designed to provide needed information for the skeleton fitting task, by highlighting marker sites that undergo important relative motion

with respect to the underlying bones. It also helps to eliminate redundant markers and identify potentially interesting new marker locations.
The paper focuses first on the problem of skeleton identification for motion capture. Then it recalls our local fitting technique for deriving joint center from relative marker trajectories. The next section illustrates how it can be used to optimize the marker positioning of the upper-torso region. The conclusion summarizes the trade-offs regarding marker positioning and suggests new research directions.

## 2 Related Work

Identifying the correct location of human joint center from external information is a difficult problem. The most simple approach is to scale a standard human skeleton to the total height of a given person; needless to say, it requires some adjustments but it is sufficient for entertainment applications [2]. Within the same frame of mind, external anatomic features can be detected and exploited from a static 3D envelop captured by digital cameras [3]. However, the precision of these two approaches is very low.
Other promising techniques emerge from the field of video-based motion analysis [4]. In [5] an arm recorded with a stereo system is being tracked by fitting a model built out of ellipsoids to the data. This way, the skeleton fitting is concomitant to the motion tracking. In the longer term, one should be able to derive a generic model of the skin deformation from such data, thus paving the way to much more precise identification of the underlying skeleton movements.
Presently optical and magnetic systems prevail in motion capture as they offer the best compromise in terms of precision and overall cost (processing and human intervention). It is a standard working hypothesis in the literature to assume that the markers are rigidly linked to the underlying skeleton [6] (it is also reported for magnetic motion capture [7], [8]). However, the rigid body hypothesis causes important errors in the estimation of the joint kinematics. This was reported in [9] for marker-based systems or in [2] for magnetic systems. It is difficult to identify a better model for the local movement of the markers as it results from the combination of the inter-related movements of the bones, muscles, fatty tissues and the skin. Proposed solutions in optical motion capture are: carefully designing marker clusters [10], considering each marker separately [11], or allowing partial freedom of motion between the markers and the associated bones [12]. This latter work proposes a methodology based on an anatomic human model. The human model encompasses a precise anatomic description of the skeleton mobility associated with an approximated envelope. It has a double objective: by ensuring a high precision mechanical model for the performer, the tracking algorithm can predict the 3D location and the visibility of markers. This reduces significantly the human intervention in case of marker occlusion. The work described in the present article exploits the visualization features of a local fitting tool for which we recall the major characteristics in the next section (we refer the reader to [13] for full details).


a
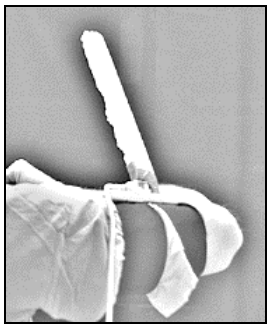
b

**Fig. 1**: Orientation error between a strapped magnetic sensor and the underlying arm during axial rotation. A dedicated approach solving for this problem is proposed in [2] for magnetic motion capture

## 3. Building Local Frames

When looking for the position of the bones of a person, a first observation is that the relative distance of markers attached to one limb is almost constant. The biggest deviations occur when markers are attached on parts that suffer maximal deformation during the movement, as around the joints or on massive muscles (e.g. on the thigh). Our approach handles this context by decomposing the problem into two tasks: the partitioning of markers into rigid *cliques* and the estimation of joint centers. A *clique* denotes a set of markers where each member remains within a distance tolerance wrt all the other markers of the set. Mastering the partitioning and the joint center estimation allows us to visualize local marker trajectories and thus better understand the skin deformations

### 3.1 Partitioning Marker into Rigid Segment Set

In the following, we assume that we exploit a motion called the "gym motion", which highlights most of the body mobility with simple movements. The corresponding file of 3D marker locations is the input of the *partitioning* algorithm.
The partitioning algorithm computes the distances between markers at each frame of the gym motion (**Fig. 2**). It selects the biggest cliques for a given distance threshold. This condition defines a rigid segment set. The system may look for the expected number of partitions or the user can interactively tune this threshold (**Fig. 3**). In addition, we define the *attachment weight* of a marker to a segment as a normalized measure of the rigidity of its attachment to that segment. By default, all the attachment weights have a value of 1.0.

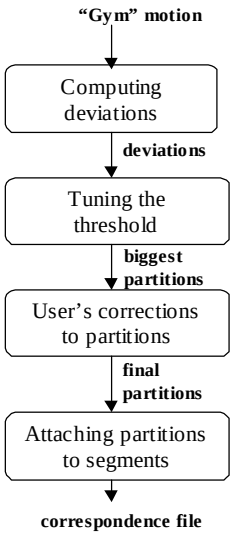


**Fig. 2.** Partitioning algorithm

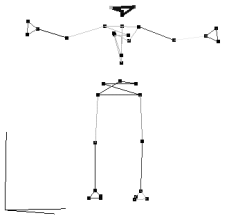

**Fig. 3.** Partitions after user corrections

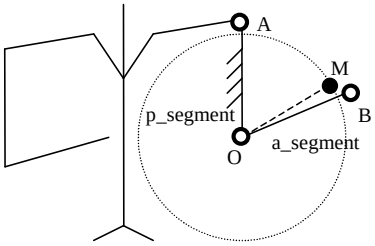


**Fig. 4.** The trajectory of a marker M around an adjacent segment OA

### 3.2 Visualizing Relative Trajectories of Markers

If we consider a referential bound to a bone represented by a segment e.g. OA (**Fig. 4**), the markers that are attached on adjacent segments (e.g. OB), theoretically move on a sphere centered on the joint that links the two segments (here joint O). This comes from the hypothesis of constant distance between markers and joints.
The position of a 3D object in space is completely defined by three non-colinear points. Thus, if we have a minimum of three markers on a segment, we can define the position and orientation of that object in space. Afterwards, we compute the movement of the markers on adjacent segments in the referential established by these markers and we estimate their centers of rotation (as in **Fig. 5** and **Fig. 6**). The centers of rotation correspond to the joints. From their position in space, we can approximate the lengths of the body segments as the distances between them. For example, in **Fig. 4** we can compute the position of the joints A and O in space and we get the distance ||AO||.

Due to the deformations undergone by the skin during the motion, the markers attached on a limb change their position with respect to the bone. As long as the deformation is only due to a twisting along the bone segment, it is filtered out by its property of maintaining the distance to the joints. However, a deformation that is changing the distance to the bone (e.g. due to muscles such as biceps) or one that changes the position along the bone induces unknown errors for the joint center computation. Markers suffering such deformation errors are further said to belong to the *noisy*

*class*. We deal with these errors by introducing a LSQ computation of the center of rotation. We use a modified version of the Levenberg-Marquardt method [14] for all of our least squares computations. Depending on the complexity of the movements, the errors sum up or compensate each other (more details in [13]).

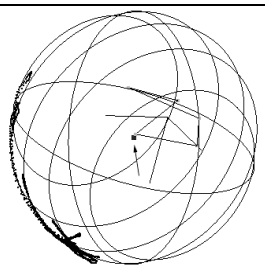

**Fig. 5.** Estimating the center of rotation of a marker

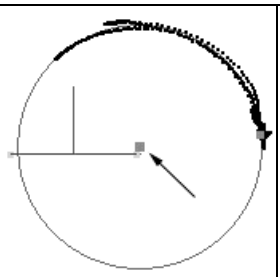

**Fig. 6.** The segment can be determined by only 2 markers

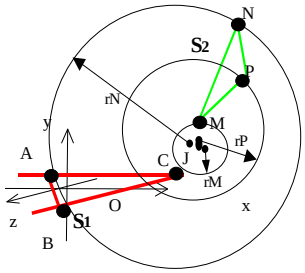


**Fig. 7.** Weighting centers of rotation for different markers on segment $S_2$

### 3.3 Estimating the Position of Joints

In the p_segment referential we compute all the centers of rotation for all the markers of an adjacent segment *a_segment* (**Fig. 4**). The center of rotation is estimated as the result of the function:

$$\arg\min_{r,x_0,y_0,z_0} \sum_{trajectory} (d(r,x,y,z) \times weight(r,x,y,z))^2 \quad (1)$$

corresponding to the LSQ minimization [10] of the function:

$$d(r,x,y,z) \times weight(r,x,y,z) \quad (2)$$

where:

$$d(r,x,y,z) = \sqrt{(x-x_0)^2 + (y-y_0)^2 + (z-z_0)^2} - r \quad (3)$$

and the function $weight(r,x,y,z)$ computes the inverse of the density of the trajectory samples in a region of the space. We compute this density by first dividing the space in a set of parallelepipeds in which we count the number of points. First we compute automatically the minimal box containing all the points of the trajectory and we divide it, dividing each direction by a factor of 5 or 10. This increases the importance of poorly populated regions of the space, where the performer stays for very short time.

We then estimate the joint position as the center of mass of the centers of rotation, weighted by the associated marker weight (**Fig. 7**).

$$weight_{center} = weight(mkr, a\_segment)\, factor(mkr, a\_segment) \quad (4)$$

In our experiments, we found a good value for factor given by:

$$factor(mkr, a\_segment) = 1 \Big/ radius(mkr, p\_segment) \quad (5)$$

Let us take **Fig. 7** as an example. After defining the system of coordinates bound to $S_1$, we estimate the center of rotation J of $S_2$ in this referential. In order to do this, we estimate the center of rotation $\bar{x}_J$ of each of the markers M, N and P. Then we compute the mass center of the centers of rotation for M, N and P using the weights computed with the previous formula:

$$\bar{x}_J = \frac{\sum_{centers} (\bar{x}_{center} \times weight_{center})}{\sum_{centers} weight_{center}} \quad (6)$$

There is a case where the trajectory of a marker describes a circle and not a sphere, due to reduced degree of freedom for a certain joint (namely the elbow). We project this trajectory in the plan that best contains it. This plan can be found by using a LSQ that minimizes the distance between it and the points on the trajectory (**Fig. 6**).

A certain attention has to be paid to the case where we have less than three attached markers on a segment. This case occurs often in our experiments. Currently, we are satisfied with two markers if the adjacent joints can be acceptably modeled as having only one rotational degree of freedom. In this case we determine the system of coordinates by the plane that contains the two markers of the base segment and the marker whose trajectory is being tracked. The center of rotation is computed in this plane and then mapped back into the global referential. We compute there the center of mass of all the centers of rotation, computed for all the markers on a neighbor segment in order to find an estimate for the position of the joint. Afterwards, we perform as explained before. For example (**Fig. 6**), we compute all the rotation centers of the markers on OA around OB, and all the rotation centers of the markers on OB around OA. Then we compute the center of mass using the weights of the considered markers and the inverse of the radius of the circles or spheres described by them during their motion.

## 4. Optimizing Marker Position

We propose to exploit the visualization of markers' local trajectories to get more insight into the bone/skin relationship. The tool should allow us to:

- make decisions relative to the inclusion of a bone in the skeleton model,
- distinguish between bone movement, muscle mass deformation and skin sliding,
- discover artifacts due to underlying bone movements,
- appreciate the correlation between bone configuration and marker position.

We have chosen to illustrate the marker position optimization on a difficult case-study to better stress the interest of the visualization tool. We have retained the up-down (shrugging) and the forward-backward motions of the clavicles. The first part of the study focuses on the relation between partitioning and marker trajectory analysis. The visualization tool allows the assessment of the marker locations with the objective of retaining pertinent ones while eliminating others. The second part of the study highlights the skin sliding in the back region.

### 4.1 Test-Case Marker Set and Motion

Fig. 8 shows the proposed marker set on the spine and thorax (the image is inverted to remove the black background). All the useful markers have a label according to the following convention. The names of markers on the **back** start with **B**. Those on the spine have a format $\mathbf{B}_i$ with i equal 1, 2 (lumbar), 3,4 (thoracic) and 5 (neck base). Two other markers on the thorax are labeled with **BL** (as Low) and **BH** (as High). The names of markers on the **front** start with **F** respectively with **F1** and **F3** on the clavicles joints and **F2**, **F4**, **F5** on the thoracic cage. The distance F4-F5 is approximately 30 cm. Finally the names of markers on the shoulders start with **S** respectively with **SR** for Right side and **SL** for Left side. Compared to standard motion capture practice [1], the present set of makers is deliberately large to explore the local skin deformations.
The motion is performed so as to highlight a single degree of mobility at a time: here the clavicle up-down (schrugging) and forward-backward motions. The motion is repeated a few times for each mobility either independently or simultaneously on both sides. The same initial posture with dangling arms is used for all motion recordings. In addition to being captured, the whole motion capture session has been recorded with a digital video camera. A selection of snapshots has been made from the resulting DVD tape and is presented below.

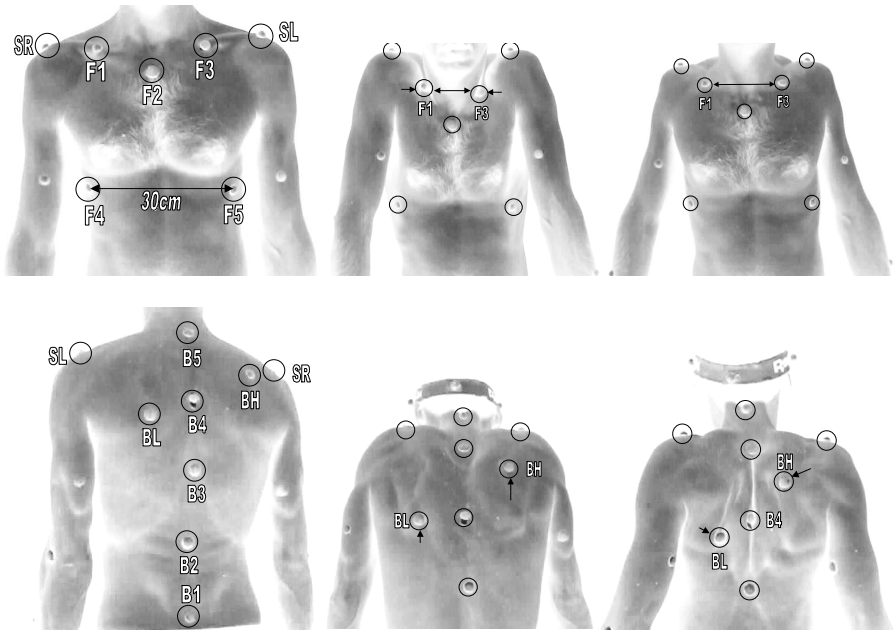


**Fig. 8.:** Front and back views of the spine and thorax regions

### 4.2 Retaining Pertinent Markers

The partitioning is the action of grouping markers belonging to the same body segment. This stage is important since it determines the local frames in which marker trajectories are further built and analyzed. Fig. 9 shows the cliques of the upper body. The thorax region is divided into three cliques (marker groups):

- the right clavicle group includes SR, F1 and BH
- the left clavicle group includes SL, F3 and BL

Thorax partition includes all the other (labelled) markers. It is relevant to include also the spine markers into this partition because the studied motion keeps the back straight.

The trajectory displayed on Fig. 10 exhibits a clear rotation behavior of the SL marker during a few shrugging motions. The center of rotation is close to the location of the F3 marker put on the left clavicle joint. Although with a short lever arm, the amplitude of the rotation is about 60°, indicating that a clavicle segment is highly relevant in a skeleton model. The 10cm scale is based on the F4-F5 distance.

When studying the motion of the SL marker, it quickly appeared that the markers on the clavicle joints were suffering strong local displacements due to the clavicle bones underlying motions. The variation of the F1-F3 distance is shown on the images of Fig. 8 and the successive drawings of Fig. 11 (indicated with arrows on (a) and (b)).

In Fig. 11 (top views) we compare the SL marker local trajectory for an alternate thorax partition that excludes the two markers F1 and F3 on the clavicle joints. Although slightly different from the previous partition case, the resulting SL marker trajectory is qualitatively similar, thus justifying the abandon of the F1-F3 markers for the thorax partition. In addition, the removed markers F1 and F3 proved to be a source of difficult 3D reconstruction as illustrated on Fig. 12 with a local rotation artifact during the forward clavicle motion.

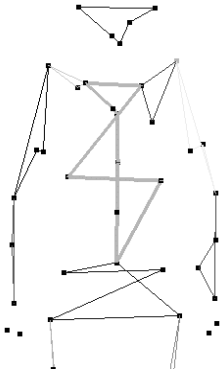

**Fig. 9.:** Initial marker partioning (front view)

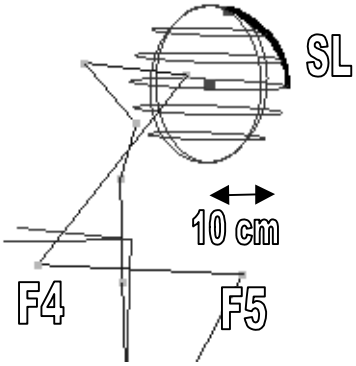


**Fig. 10**: Front view of the local trajectory of the left shoulder marker SL expressed in the thorax partition frame

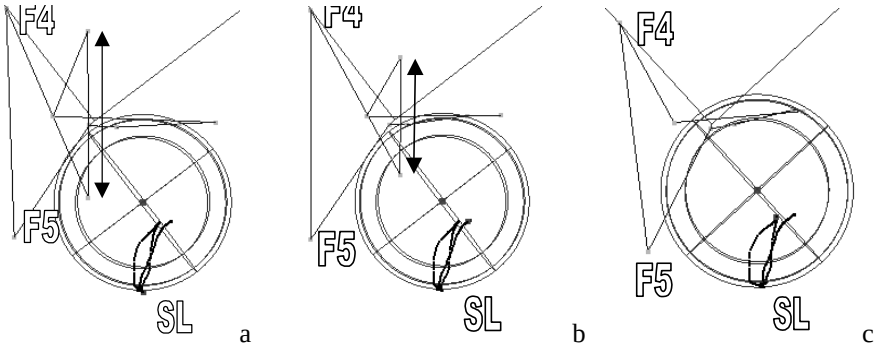


**Fig. 11**: Top view of the left shoulder marker trajectory with respect to the thorax partitions: initial partition in two postures for high clavicles (a) and low clavicles (b), and alternate partition for (c)

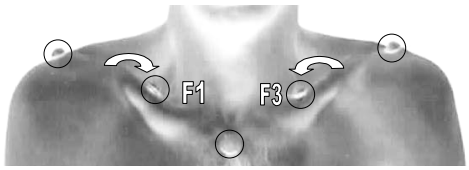


**Fig. 12**: Local rotation of F1 and F3 due to forward clavicles motion

### 4.3 Studying Local Skin Deformations

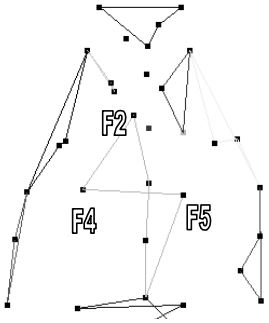


**Fig. 13**: Alternate thorax partition (without B4)

The present section focuses on markers BL and BH that are respectively on the low and high part of the muscular mass associated to the scapula motion. The major aspect in these trajectories is their translational rather than rotational nature. These characteristics have already appeared on **Fig. 8**.

A second alternate thorax partition (without marker B4) had to be defined as this marker could not be tracked during the whole sequence. The marker B4 is subject to severe deformation and pushing of muscular masses (that even led to the loss of this marker and the repetition of this motion).

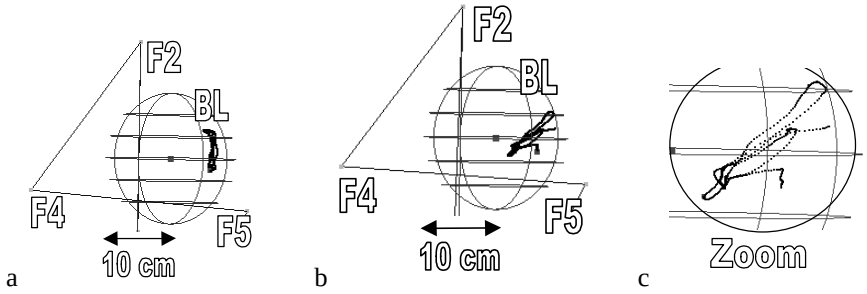


**Fig. 14**: Front views of marker BL: local trajectories during shrugging (a) and forward-backward motion (b). (c) is an enlargment of (b) trajectory

Fig. 14 explores further the translation characteristics of the markers BL and BH. Their excursion ranges are quantified based on the F4-F5 distance. What is especially noticeable is the regularity of the trajectories highlighting the high correlation between local skin deformation and underlying bone motion. However we have observed sudden displacement of the BH marker in the sagital plane (side view). This artifact possibly comes from the underlying motion of the upper part of the scapula. Unless the scapula motion is of special importance, the region of BH marker should be avoided.

## 5. Conclusion

This is only one of our first sets of experiences with the analysis of the local trajectories of the markers. The possibility to simultaneously view a movement in several

systems of coordinates, makes the decision process clear and efficient (Fig. 15). It provides pertinent feedback on the marker positioning, although highly depending on the quality of the gym motion. Our first conclusion regarding the studied region is that:

- Adding more markers (three per segment), definitely helps to improve the local fitting (by selecting and organizing the ones that lead to good estimation),
- The scapula joint seems not identifiable with the current optical motion capture methodology. We can however gain a better understanding of the region deformation.

Our results on this type of (i.e. with cyclical movements of independant degrees of mobility) suggest that, in some body regions, there is a strong correlation between skeleton motion and local skin deformation. This is in phase with some observations from Cappozzo in [9]. One approach for the identification of this correlation could be to train a dedicated neural network with the gym motion for each major body region. The result would describe how the marker moves with the skin, as a function of the current posture. Compared with the current assumption of fixed marker w.r.t the underlying bones, we believe such a *marker model* would improve the skeleton identification and the quality of the captured motion. In the near future we plan to focus on the shoulder region with more (and smaller) markers.

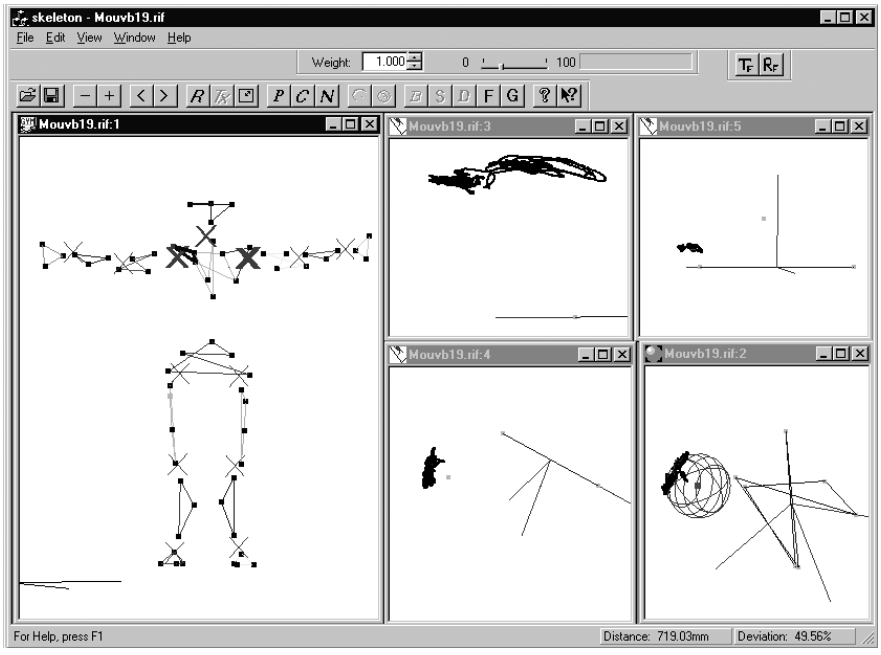


**Fig. 15:** Interface for simultaneous visualization in different frames

## 6 Acknowledgements

We thank our MOCA partner, ACTISYSTEM, for their help in providing test data files as well as our colleagues in LIG for their technical help. The MOCA project was sponsored by the European ESPRIT program. This work is also partly supported by the Swiss Federal Institute of Technology, Lausanne.

## References

1. VICON 8: The Manual. Oxford Metrix, January 1999
2. Molet, T., Boulic, R., Thalmann, D.: Human Motion Capture Driven by Orientation Measurements. Presence, MIT, Vol.8, No2, 1999, pp.187-203
3. Gray, S.: Virtual Fashion. IEEE Spectrum, Feb. 98.
4. Aggarwal, J.K., and Cai Q.: Human Motion Analysis: A Review. Proceedings, IEEE Nonrigid and Articulated Motion Workshop, June 16,1997, San Juan, Puerto Rico.
5. Fua, P., Grün, A., Plänkers, R., D'Apuzzo, N. and Thalmann, D.: Human Body Modeling and Motion Analysis From Video Sequences. International Symposium on Real Time Imaging and Dynamic Analysis, June 2--5, 1998, Hakodate, Japan
6. Veldpaus, F.E., Woltring, H.J., Dortmans, L.J.M.G.: A Least-Square Algorithm for the Equiform transformation from Spatial Marker Co-ordinates. Journal of Biomechanics, 21(1):45-54,1988
7. Bodenheimer, B., Rose, C., Rosenthal, S., Pella, J.: The Process of Motion Capture: Dealing with data. 8th EUROGRAPHICS Int. Workshop on Computer Animation and Simulation'97, Budapest, Hungary, D. Thalmann and M. van de Panne eds., ISBN 3-211-83048-0, Springer-Verlag Wien, pp 3-18.
8. O'Brien, J., Bodenheimer, R.E., Brostow, G., Hodgins, J. K.: Automatic Joint Parameter Estimation from Magnetic Motion Capture Data. Proc. of Graphics Interface'2000, pp 53-60, Montreal, Canada
9. Cappozzo, A., Catani, F., Leardini, A., Benedetti, M.G., Della Croce, U.: Position and Orientation in Space of Bones during Movement: Experimental Artefacts. Clinical Biomechanics 11(2), pp 90-100, 1996, Elsevier.
10. Cappozzo, A., Cappello, A., Della Croce, U., Pensalfini, F.: Surface-Marker Cluster Design Criteria. IEEE Trans. on Biomedical Engineering 44(12), December 1997
11. Halvorsen, K., Lesser, M., Lundberg, A.: A new Method for Estimating the Axis of Rotation and the Center of Rotation. Technical note, Journal of Biomechanics 32 (1999) 1221-1227, Elsevier.
12. Herda, L., Plaenkers, R., Fua, P., Boulic, R., Thalmann, D.: Skeleton-Based Motion Capture for Robust Reconstruction of Human Motion. Proc. of Computer Animation'2000, Philadelphia, May 2000, IEEE Press.
13. Silaghi, M-C., Plaenkers, R., Boulic, R., Fua P., Thalmann D.:Local and Global Skeleton Fitting techniques for Optical Motion Capture. (IFIP Workshop on Modelling and Motion Capture Techniques for Virtual Environments) November 26th 1998, Geneva
14. Press, W.H., Flannery, B.P., Teukolsky, S.A., and Vetterling, W.T.: Numerical Recipices, the Art of Scientific Computing. Cambridge U. Press, Cambridge, MA, 1986